Two-Dimensional Fokker-Planck Analysis of Core Plasma Heating by Relativistic Electrons

Y. Nakao [1)], T. Yokota [1)], T. Johzaki [2)], H. Nagatomo [2)], H. Sakagami [3)], K. Mima [2)]

[1)] Department of Applied Quantum Physics and Nuclear Engineering, Kyushu University, Fukuoka 812-8581, Japan
[2)] Institute of Laser Engineering, Osaka University, Osaka 565-0871, Japan
[3)] Department of Computer Engineering, University of Hyogo, Shosha, Himeji 671-2201, Japan

e-mail contact of main author: nakao@nucl.kyushu-u.ac.jp

Abstract. One of the key issues in the fast ignition scheme is a clarification of the imploded core heating by laser-produced relativistic electrons. To investigate the core heating process, we have developed two-dimensional relativistic Fokker-Planck (RFP) codes for fast electrons in dense plasmas. After describing the physics model, we first examine the feature of energy deposition of relativistic electrons injected into the dense core region. Next, on the basis of integrated simulation combining PIC, 2-D hydrodynamics and RFP codes, the possibility of fast heating of imploded core is discussed.

1. Introduction

The fast ignition (FI) is an attractive scheme for inertial fusion energy [1]. In this scheme the fast electrons, generated near the surface of pre-compressed pellet, propagate to the dense core region and deposit part of their energy there. The generation and propagation processes have been actively studied by means of PIC simulation. On the other hand, only a little has been reported about the energy deposition process.

In most of the previous studies on ignition and burn properties of fast ignition targets, the energy deposition process of fast beam particles was not explicitly treated. In Ref. [2], for example, the penetration depth of beam particles was estimated beforehand using a simple slowing-down model, and then the ignition process was simulated by assuming that the beam particles deposit their kinetic energy uniformly in the pre-determined region. For more precise analysis of ignition process, especially the time-dependence of core plasma heating, a kinetic transport model for fast electrons would be necessary.

To investigate the core heating and ignition by relativistic electrons, we previously developed a one-dimensional (1-D) relativistic Fokker-Planck (RFP) code [3]. The code was coupled with a hydrodynamics one to analyze the core heating and ignition process of compressed targets. However, because of 1-D nature of the code, its application has been limited to planar targets. More importantly, multi-dimensional effects could not be included in the code. For instance, the current density carried by fast electrons $\boldsymbol{J}_f$ in the core would reach the order of 10^{17} A/m^2, which generates the strong magnetic field mainly through $\nabla\times\left(\eta\boldsymbol{J}_f\right)$ [4] (η is the plasma resistivity), and then causes the beam pinching. To take into account these effects, a

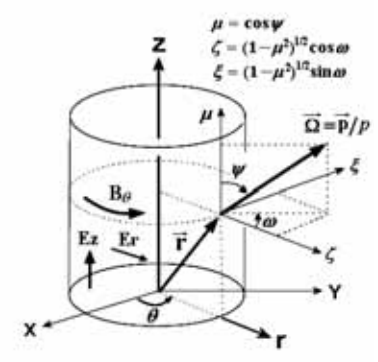

Fig.1 2-D cylindrical coordinate system.

multi-dimensional (at least 2- D in coordinate space) is indispensable. Thus, we have recently developed 2- D RFP codes to calculate fast electron transport in dense plasmas. The two codes are respectively written for a cylindrical (r- z) coordinate system with axial symmetry (**Fig. 1**) and for a planar (x- y) coordinate one.

In this paper, we first examine the multi-dimensional features of the energy deposition of relativistic electrons injected into dense core region. Then, we analyze the fast heating of imploded core, on the basis of integrated simulation combining 2-D hydrodynamics (implosion), PIC (generation of fast electrons) and RFP-hydro codes.

2. Outline of Physics Model and RFP Equation

In our core-heating model, the behavior of fast electrons is calculated using the RFP code, while the bulk plasma is treated as fluid. As for the interactions of relativistic electrons with dense background plasma, the dominant process is binary collisions in the impact parameter range $b_{min}<b<\lambda_D$. In addition, collective response of background electrons at long distance ($b> \lambda_D$), that is plasma oscillation, contributes to the energy deposition of fast electrons [5]. To describe these two effects, we modify relativistically [6] the FP collision term and the Lenard- Balescu one.

The 2-D RFP equation in the coordinate system shown in Fig. 1 is written as follows:

$$\frac{\partial f}{\partial t}+\frac{p}{\gamma m_e}\left[\mu\frac{\partial f}{\partial z}+\sqrt{1-\mu^2}\cos\omega\frac{\partial f}{\partial r}-\frac{\sqrt{1-\mu^2}}{r}\sin\omega\frac{\partial f}{\partial \omega}\right]$$
$$+\left[F_z\mu+F_r\sqrt{1-\mu^2}\cos\omega\right]\frac{\partial f}{\partial p}-F_r\frac{\sin\omega}{p\sqrt{1-\mu^2}}\frac{\partial f}{\partial \omega}+\left[F_z\left(1-\mu^2\right)-F_r\sqrt{1-\mu^2}\cos\omega\right]\frac{1}{p}\frac{\partial f}{\partial \mu} \qquad (1)$$
$$=\left(\frac{Y_e n_e}{m_e}+\frac{Y_i n_i}{m_i}\right)\frac{m_e^2}{p^2}\frac{\partial}{\partial p}\left(\gamma^2 f\right)+\frac{1}{2}\left(Y_e n_e+Y_i n_i\right)\frac{m_e}{p^3}\left[\frac{\partial}{\partial \mu}\left\{\gamma\left(1-\mu^2\right)\frac{\partial f}{\partial \mu}\right\}+\frac{\gamma}{1-\mu^2}\frac{\partial^2 f}{\partial \omega^2}\right]+S$$

with

$$Y_j=4\pi\left(Z_j e^2/4\pi\varepsilon_0\right)^2\left(\ln\Lambda_{binary}+\ln\Lambda_{collective}\right)\quad (j=e,i), \qquad (2)$$

$$F_z=(-e)\left(E_z+B_\theta p\sqrt{1-\mu^2}\cos\omega/\gamma m_e\right), \qquad (3)$$

$$F_r=(-e)\left(E_r-B_\theta p\mu/\gamma m_e\right), \qquad (4)$$

$$\ln\Lambda_{binary}=\frac{1}{2}\left\{\ln\frac{1}{2}\left(\frac{2\lambda_D}{\lambda\!\!\!^{-}_{DB}}\right)^2+\frac{1}{8}\left(\frac{\gamma-1}{\gamma}\right)-\frac{(2\gamma-1)}{\gamma^2}\ln 2+1-\ln 2\right\}, \qquad (5)$$

$$\ln\Lambda_{collective}=\frac{1}{2}\ln\frac{2}{3}\left(\frac{p}{m_e\lambda_D\omega_p}\right)^2-\frac{1}{2}, \qquad (6)$$

where $f(r, z, p, \mu, \omega, t)$ is the distribution function of fast electrons, γ is the Lorentz factor, n_e (or n_i) is the number density of the bulk electrons (or ions), $S(r, z, p, \mu, \omega, t)$ is the fast electron source, μ is the directional cosine of the momentum vector $\boldsymbol{p}$ relative to z-axis and ω is the angle between the planes formed by $\boldsymbol{p}$ and $\hat{\boldsymbol{z}}$ vectors and by the $\hat{\boldsymbol{z}}$ and $\hat{\boldsymbol{r}}$ vectors; $\hat{\boldsymbol{z}}$ and $\hat{\boldsymbol{r}}$ are unit vectors in z and r directions, respectively. The Coulomb logarithm for binary collisions $\ln\Lambda_{binary}$ is obtained using the Mϕller's cross-section in the FP theory, while that for the collective plasma response $\ln\Lambda_{collective}$ is derived by assuming $\varepsilon(\boldsymbol{k}, \omega) = 1- \omega_p^2 / \omega^2$ in the Lenard-Balescu equation.

The fast electrons injected into the core plasma induce electric and magnetic fields there. The evolution of these fields are evaluated by combining generalized Ohm's law, the Ampere-Maxwell equation, Faraday's law and the equation for total current density $\boldsymbol{J} = \boldsymbol{J_f} + \boldsymbol{J_b}$ ($\boldsymbol{J_b}$: the current density carried by the bulk electrons). Neglecting non-dominant terms in Ohm's law, we obtain

$$\boldsymbol{E} = -\eta \boldsymbol{J}_f + \frac{\eta}{\mu_0} \nabla \times \boldsymbol{B}, \tag{7}$$

$$\frac{\partial \boldsymbol{B}}{\partial t} = -\nabla \times \left(\frac{\eta}{\mu_0} \nabla \times \boldsymbol{B} \right) + \nabla \times \left(\eta \boldsymbol{J}_f \right), \tag{8}$$

where μ_0 is the permeability of free space. Assuming rotational symmetry, we evaluate the fields $E_z(r, z)$, $E_r(r, z)$ and $B_\theta(r, z)$.

The energy deposition rate of fast electrons consists of the energy loss rates $P_B + P_C$ due to binary collisions and excitation of collective response, and the Joule heating rate P_J through return current, i.e. $P_{dep} = P_B + P_C + P_J$. These rates are evaluated by

$$P_B + P_C = -\int m_e c^2 (\gamma - 1) \left[\left(\frac{Y_e n_e}{m_e} + \frac{Y_i n_i}{m_i} \right) \frac{m_e^2}{p^2} \frac{\partial}{\partial p} \left(\gamma^2 f \right) \right] dp^3, \tag{9}$$

$$P_J = \eta \left(J_{b,r}^2 + J_{b,z}^2 \right), \tag{10}$$

where $J_{b,r}$ (or $J_{b,z}$) is the component of return current density in the r (or z) direction. The return current density is calculated by

$$\boldsymbol{J}_b = -\boldsymbol{J}_f = e \int \frac{\boldsymbol{p}}{\gamma m_e} f \, d^3 \boldsymbol{p}. \tag{11}$$

By coupling the above heating process with hydrodynamic behavior of the bulk plasma, it becomes possible to evaluate the ignition conditions more realistically than before [2, 3].

3. Energy Deposition of Relativistic Electrons in Dense Plasma

In order to examine the properties of the core heating by fast electrons, we carried out the transport simulations for mono-energetic (E_0=0.5~2MeV) electron beams injected continuously from the base of a uniform cylindrical DT plasma (ρ=300g/cm^3, T_0=0.2keV, z_{max}=50μm, r_{max}=25μm). The source electrons are directed forward and assumed to have a Super-Gaussian intensity distribution with a perk value of I_{max}=0.5~3×10^{20}W/cm^2 on the z-axis and a HWHM (Half Width at Half Maximum) of 15μm.

Figure 2 shows contours of (a) the magnetic field B_θ generated around the beam axis and (b) energy deposition rate at t = 1ps for the case of E_0=1MeV and $I_{\max}$=1×10^{20}W/cm^2. For the purpose of comparison, the energy deposition rate at the same timing for the case neglecting the field effects is also shown in Fig.2 (c).
Under the present condition, the current density formed by the injected fast electrons $J_{f,z}$ is more than 10^{17}A/m^2, and B_θ grows about 700Tesla at maximum. In the case of Super-Gaussian beam injection as considered here, strong magnetic field is generated only near r~HWHM. This is because the evolution of B_θ is most dominated by $\partial J_{f,z} / \partial r$. Because of this magnetic field, the beam electrons are pinched toward the beam axis and the energy deposition rate is locally enhanced near r~HWHM. In the present case the core plasma temperature reaches 3.2keV at maximum at t = 1ps.

It was also found that the self-generated electric field shortens the penetration of the beam electrons into the plasma. In the present case, the power fractions of P_B, P_C and P_J to the total energy deposition rate are respectively 50%, 40% and 10% at 0.1ps (the maximum value of ion temperature is 0.45keV at this moment), and 54%, 42% and 4% at 1ps. Thus, it is indispensable to consider the contribution of the collective response effect when evaluating the core-heating rate. In addition, when the core temperature is lower than 1keV, the Joule heating via return current is not negligible because $\eta \propto T^{1.5}$.

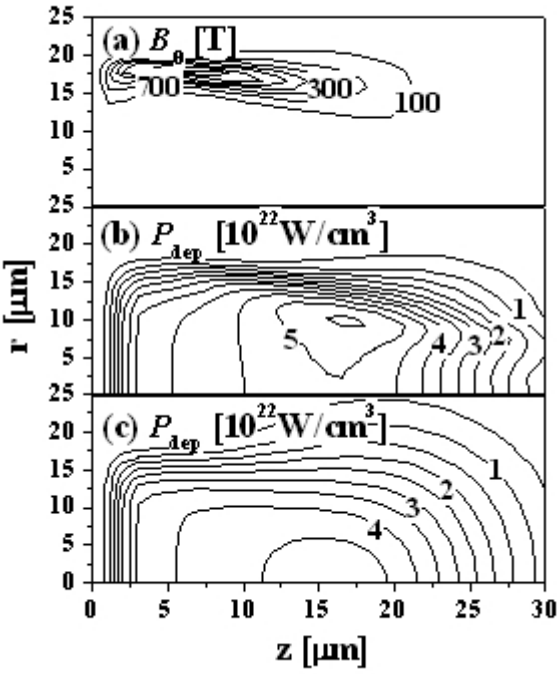

Fig. 2 Spatial profiles at t = 1ps of (a) magnetic field B_θ, (b) energy deposition rate P_{dep} and (c) P_{dep} for the case neglecting field effects. The fast electron current passes in the negative z direction, determining the direction of B_θ.

These effects resulting from the self-generated fields and the collective plasma response would be favorable from the viewpoints of efficient core plasma beating in fast ignition.

4. Imploded Core Plasma Heating by Fast Electrons

Previously, using a 1-D RFP code coupled with 1-D radiation hydro code, we evaluated the core heating properties of the recent integrated experiments for cone-guided targets [7, 8] and showed a quite important role of the relatively low energy component ($E_0 \leq 1$MeV) of electron beam [9]. However, in the previous study, a 1-D planar geometry was assumed, and implosion and fast electron generation processes were not included. For understanding the physics phenomena and proving fusion burning in the FI scheme, multidimensional overall calculation including the implosion dynamics, generation of fast electrons in relativistic laser-plasma interactions, core heating, and fusion burning is indispensable. Recently, we have started "Fast Ignition Integrated Interconnecting code project" (FI^3 project) [10], where the each phenomenon is simulated with individual code and the each code is collaborating with the others through the data transfer.

In the first step of the FI^3 project, we carried out the integrated simulations for analysis of the integrated experiments for the cone-guided targets [7,8] and examined the implosion dynamics, the fast electron generation, and the core heating [11]. First, the 2-D Arbitrary Lagrangian Eulerian - Constrained Interpolation Profile (ALE – CIP) radiation -hydro code "PINOCO" [12] simulates the implosion process to evaluate the core plasma profile at the maximum compression. Using this profile, the 1-D collective Particle In Cell (PIC) code "FISCOF1"[13] evaluates the time-dependent energy distribution of fast electron generated by the relativistic laser-plasma interactions. Finally, on the basis of a 2-D coupled Eulerian hydrodynamics and the RFP code, the core heating process are simulated using both profiles

(the imploded core plasma and the fast electrons). As the result of the core heating simulation using the fast electron profiles in the Au cone obtained from 1-D PIC simulation (300fs Gaussian pulse, wavelength λ_L = 1.06μm and maximum intensity $I_L = 10^{20}$W/cm^2), the core plasma temperature is slightly increased. This is because the electron energy is too high to heat core and the laser pulse duration is shorter than that at the experiments.

One of the possible mechanism to slow down the fast electrons, neglected in the previous evaluation, is the effect of density gap at the contact surface between the cone tip and the imploded plasma [14]. The fast electrons generated at the inner surface of the cone pass through the cone tip and then come into the imploded plasmas. The bulk electrons in the imploded plasma behind the cone tip form the return current to keep the current neutrality. If the bulk electron density is comparable to the injected fast electron density, the drift speed of bulk electrons becomes close to light velocity. Thus, the microinstabilities such as two-stream instability and the Weibel instability occur, which slow down the fast electrons. In addition, such microinstabilities inhibit also the return current flow, so that the strong static field will be build up at the contact surface. The static field will confine some fractions of the fast electrons inside the cone tip. Such a situation will be realized in the implosion of the cone-guide targets. In the present study, we estimate the core heating properties by considering the density gap effect.

4.1 Imploded core profiles

First, we carried out the implosion simulation for a cone-guided target with "PINOCO". A target shell of polystyrene (ρ = 1.06 g/cm^3) has a uniform thickness of 8μm and an inner radius of 250μm. The cone with an opening angle of 30 degree is attached to the shell. The target is uniformly irradiated by the 6 kJ (on target) Gaussian-pulse-shaped laser with λ_L = 0.53 μm. **Figure 3** shows the imploded core profiles at 1.93 ns when the maximum average ρR was measured. This profile was used for the following core heating analysis.

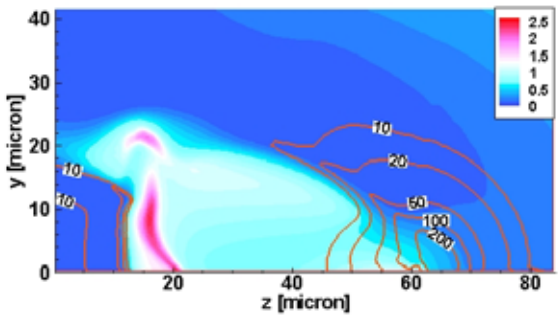

Fig. 3 Imploded core profiles at t = 1.93 ns when the maximum average ρR is measured. The contours show the density [g/cc] and the color map shows the ion temperature [keV].

4.2 Energy spectrum of laser-produced fast electrons

The profiles of fast electrons generated in the laser-plasma interaction were evaluated with 1-D PIC code "FISCOF1". The Au cone tip was modeled by the 10μm-thickness plasma with electron density $n_e = 100n_c$ (n_c is the critical density). The 50μm-thickness imploded plasma was putted behind the cone tip. The simulations were carried out by assuming that the electron density in the rear of cone tip is $n_{e,rear} = 100n_c$ and $2n_c$. The forward-directed fast electrons were observed at 10μm behind the cone tip every 20fs. The 150 fs Gaussian pulse (λ_L = 1.06 μm, $I_L = 10^{20}$ W/cm^2) was assumed as ignition laser.

The temporal profiles of (a) intensity and (b) average energy of forward-directed fast electrons observed for both cases ($n_{e,rear} = 100n_c$ and $2n_c$) are plotted in **Fig.4**. The intensities become maximum at t ~ 400fs in both cases. The peak intensities are 1.6×10^{19} and

1.2×10^{19}W/cm^2 for the cases of $n_{e,rear}$ = 100n_c and 2n_c, respectively. The energy distribution of electron beams at this moment consists of two components; the temperature of higher energy component is T = 5.0MeV (slope temperature, *i.e.* $f(E) \propto \exp(-E/T)$) for both cases, while the temperature of lower energy one is 1.2MeV when $n_{e,rear}$= 100n_c and 1.5MeV when $n_{e,rear}$= 2n_c. Part of fast electrons with relatively low energy ($E \leq$ a few MeV) are confined inside the cone tip by the static field formed at the contact surface, causing the differences in the peak intensity and in the temperature of low energy component between two cases. The average energy of fast electrons $\langle E_{fe} \rangle$ is hence higher in the case of $n_{e,rear}$= 2n_c. ($\langle E_{fe} \rangle$ = 2.7MeV for $n_{e,rear}$= 100n_c and $\langle E_{fe} \rangle$ = 3.6MeV for $n_{e,rear}$= 2n_c.) After t = 400fs, the beam intensities decrease with time. However, after finishing laser irradiation (t > 700fs), the forward-directed electron beam with almost constant intensity of ~10^{18}W/cm^2 is still observed. (The intensity is lower by one order of magnitude than the peak value.) This is because the electrons confined inside the cone tip are continuously released from there. The energy distribution of the fast electrons at this moment differs from that at the peak intensity; no high energy component (E > 5MeV) exists and the averaged energy is ~ 0.5MeV. In the case of $n_{e,rear}$ = 100n_c, the intensity is lower than that for $n_{e,rear}$ = 2n_c case by one order of magnitude. The time-averaged fast electron energies are 2.16MeV for $n_{e,rear}$ = 100n_c case and 1.48MeV when $n_{e,rear}$ = 2n_c, *i.e.* 30% reduction due to the density gap effect. The energy coupling from the ignition laser to the forward-directed fast electrons is slightly high in the case of $n_{e,rear}$ = 2n_c (21.6%) compared with the case of $n_{e,rear}$ = 100n_c (19.8%).

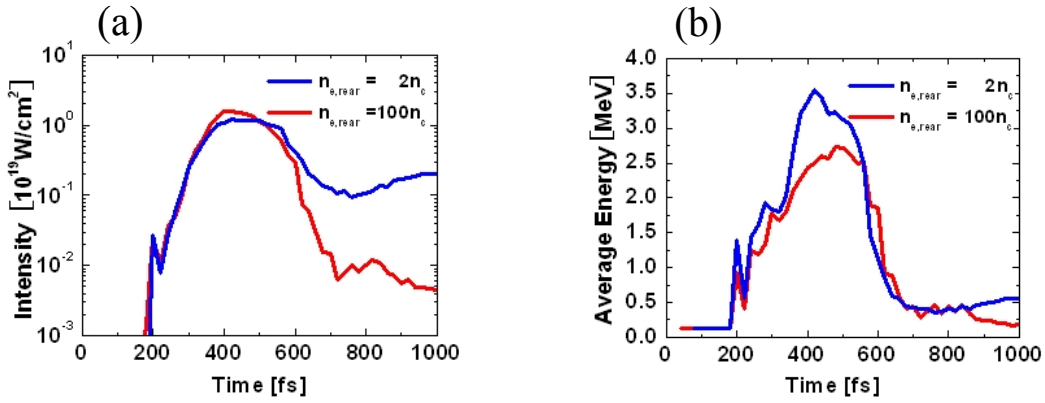

Fig. 4 Temporal profiles of (a) intensity and (b) averaged energy of observed forward-directed fast electrons for both cases ($n_{e,rear}$ = 100n_c and 2n_c).

4.3 Simulation of imploded core heating

Using the results of the implosion simulation (shown in Fig.3) as an imploded-core profile, and the time-dependent momentum distribution of fast electrons evaluated by the PIC simulations (shown in Fig.4) as the fast electron source, we evaluated the core heating properties. The fast electron source was injected behind the cone tip by assuming the super Gaussian profile with 20μm width. The duration of the ignition laser assumed in the PIC simulations are shorter than experimental values (500~900fs). In addition, the laser-plasma interaction at the sidewall of the cone was not included in the 1-D simulations. Thus, the pulse duration and energy of the fast electron beam estimated above are so smaller than those expected in the experiments. To fit the source condition to the experiment, we made an artificial correction to the fast electron profile; (a) the fast electron duration was lengthened by a factor of five, and then (b) the fast electron intensity was adjusted so that the amount of

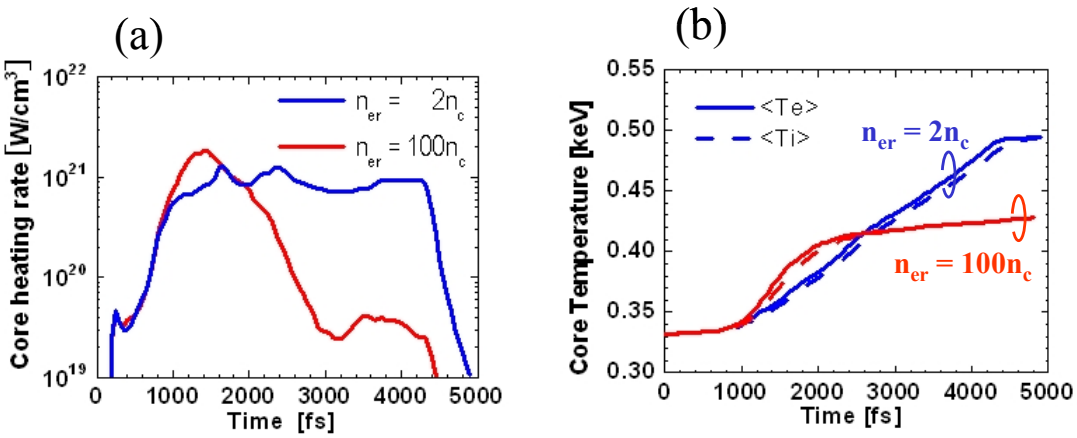

Fig 5. The temporal profiles of (a) core heating rates and (b) ion and electron temperatures averaged over the dense core region ($\rho > 50$ g/cc).

"injected source electron energy" divided by the "energy coupling from laser to fast electron η_{Le} (estimated in PIC simulations)" is equal to the laser energy E_L in the experiments (here, we adopted E_L = 300J).

The temporal profiles of (a) core heating rates and (b) ion and electron temperatures averaged over the dense core region ($\rho > 50$ g/cc) are plotted in **Fig.5**. The blue line shows the result for the case considering the density gap effect behind the cone tip, while the red line represents the case neglecting that effect, respectively. In Fig.5, the time t was set to be 0 at the beginning of electron beam pulse.

In the case including the density gap effect, due to the lower beam intensity and higher averaged energy of electrons in the early stage of core heating ($t < 2000$fs), the core heating rate and the resultant temperature rising rate are lower than in the case neglecting that effect. However, the core heating duration is longer. This is because the fast electrons with relatively low-energy, confined inside the cone tip, continue to be released from there after finishing laser irradiation. As the result, the core temperature becomes ~16% higher in the case including the density gap effect. In this case, the energy coupling efficiency from the fast electrons to the dense core is estimated to be 25%, and then the coupling from the laser to the core is 5.4%. The core plasma is heated up to 0.5keV, which is still lower than the temperature of ~0.8keV observed in the experiments [7, 8].

5. Concluding Remarks

We have examined multi-dimensional features of the transport and energy deposition of fast electrons in dense plasmas by means of relativistic Fokker-Planck (RFP) calculations. Important and favorable effects resulting from self-generated electromagnetic field and collective plasma response were demonstrated.

In the latter part of the paper, we have shown the outline of the FI^3 project and the results of integrated simulations for the recent core heating experiment for cone-guided targets [7,8]. Considering the density gap at the contact surface between the cone tip and the imploded plasma, we estimated the fast electron profiles with 1-D PIC simulations. It was found that

due to the density gap, the energy of forward-directed fast electrons becomes lower and the pulse duration becomes longer, which leads to high coupling efficiency from the fast electrons to the dense core, compared with the case neglecting the density gap effect. (Note that this effect depends on the density ratio of fast electrons to bulk electrons. When the bulk electron density is sufficiently higher than that of fast electrons, we can not expect this effect.) Even though the density gap effect is included, however, in the present simulations we could not obtain expected core heating. For more realistic estimations, each of the codes is required the model improvement, *e.g.* considerations of a) magnetic field generation during implosion, b) multi-dimensional effect in the fast electron generation, and c) re-circulation of fast electrons due to the sheath field generated around the core.

Acknowledgements

This work was performed under the collaboration program of the Institute of Laser Engineering, Osaka University and supported by MEXT, the Grant-in-Aid for Creative Scientific Research (15GS0214).

References

[1] M. Tabak, *et al.*, *Phys. Plasmas*, **1**,1626 (1994); S. Nakai, K. Mima, *Rep. Prog. Phys.*, **67**, 321 (2004).
[2] S. Atzeni, *Phys. Plasmas*, **6**, 3316 (1999).
[3] T. Johzaki, *et al.* , *Fusion Sci. Technol.*, **43**, 428 (2003); Y. Nakao, *et al.*, *Proc. of 19th IAEA Fusion Energy Conf. (Lyon, 2002)*, IAEA-CSP-19/CD, IF/P-08 (2003).
[4] J. Bell, *et al.*, *Phys. Rev. E.*, **58**, 2471 (1998).
[5] C. Deutsch, *et al.*, *Phys. Rev. Lett.*, **77**, 2484 (1996).
[6] B.J. Braams, C.F.F, Carney, *Phys. Fluids*, **B1**, 7 (1989).
[7] R. Kodama, *et al*., *Nature*, **412**, 798 (2001).
[8] R. Kodama, *et al*., *Nature*, **418**, 933 (2002).
[9] T. Johzaki, *et al*., *Annual Progress Report 2002,* ILE, Osaka University, 95 (2003).
[10] Sakagami, H. *et al*., *Proc. of 2nd Int. Conf. on Inertial Fusion Sciences and Applications (Kyoto, 2001)*, Elsevier, 380 (2001).
[11] T. Johzaki, *et al*., "*Integrated Simulations for Fast Ignition Targets*", to be published in *Proc. of ITC-13, Special issue of the Journal of Plasma and Fusion Research*.
[12] H. Nagatomo, *et al*., *Proc. of 2nd Int. Conf. on Inertial Fusion Sciences and Applications (Kyoto, 2001)*, Elsevier, 140 (2001).
[13] H. Sakagami, *et al*., *Proc. of 3rd Int. Conf. on Inertial Fusion Sciences and Applications (Monterey, 2003)*, American Nuclear Society, 434 (2004).
[14] H. Sakagami, *et al*., "*Integrated Fast Ignition Simulation of Cone-Guided Target with Three Codes"*, to be published in *Proc. of ICPP2004*.